

PAPER • OPEN ACCESS

Modelling of grid-following current-controlled VSC

To cite this article: E Saad *et al* 2023 *J. Phys.: Conf. Ser.* **2616** 012037

View the [article online](#) for updates and enhancements.

You may also like

- [Modeling and Reliability Constraint Analysis of MMC Valve](#)
Shuaiqing Wang, Shuai Chen, Yongjie Hu et al.
- [Standardization of clinical protocols in oral malodor research](#)
Ken Yaegaki, Donald M Brunette, Albert Tangerman et al.
- [Improvements for volume self-calibration](#)
Bernhard Wieneke

PRIME
PACIFIC RIM MEETING
ON ELECTROCHEMICAL
AND SOLID STATE SCIENCE

HONOLULU, HI
Oct 6–11, 2024

Abstract submission deadline:
April 12, 2024

Learn more and submit!

Joint Meeting of
The Electrochemical Society
•
The Electrochemical Society of Japan
•
Korea Electrochemical Society

Modelling of grid-following current-controlled VSC

E Saad, S Helmy, Y Elkoteshy and U Abouzayed

Electrical Power and Energy Department, Military Technical College, Cairo, Egypt
elsayed3d@gmail.com

Abstract. The voltage sourced converter (VSC) is a basic element in the grid connected solar-PV system that used in converting the DC-generated power from the solar-PV to AC power compatible with the utility grid. In this paper, a grid connected, three phase, two level VSC model and its control technique are simulated. The switched model of a three phase, two level VSC with active and reactive power controller is employed. The VSC's control is performed based on the grid following VSC methodology. In order to control the transferred active and reactive power between the VSC and the grid, a current control mode (CCM) in dq0 frame is used and discussed in the following sections. The mathematical models of all elements of control loops are developed. Furthermore, the design of these control components is presented with their performance curves using PSCAD /EMTDC software.

1. Introduction

The solar-PV systems are the most attractive and fastest growing renewable energy resource since solar energy is available anywhere [1]. Basically, the grid-connected solar-PV system consists of: (1) solar-PV modules, (2) DC-DC converter for MPPT, (3) grid-connected VSC, (4) power meter and a load that connected to the grid (if found) [2]. The VSC is considered the core of the grid-connected solar-PV system, as it converts the extracted solar-PV DC power into AC power which is used to feed the local loads or the utility grid [3]. The grid-following VSC is a combination between the VSC model and the utility grid model including the connection between them as shown in the following schematic diagram of figure1[4]. The two-level three-phase VSC consists of three similar half-bridge inverters [5]. Every phase of the VSC is tied with the utility grid through a line with a series R-L impedance. In this paper the CCM is simulated, in which the control of the instantaneous active and reactive-power is proceeded using the VSC line current's phase shift and amplitude simultaneously. Due to the dependence on the VSC line currents in control and regulation scheme, the system is protected from the over-current or faults problems. This control approach is characterized by its high accuracy in controlling the current and its high performance in dealing with harmonics [6]. For these reasons, it's preferred to be chosen and implemented in the presented system model. The system and its control loops are presented using PSCAD /EMTDC software.

2. System Parameters

The grid-following VSC system is composed of a DC source, DC capacitor-link, Two-level three-phase VSC and the utility grid model as clarified in figure 1.

2.1. DC source

In this model, a 50 kW solar-PV system was modelled. It consists of 16 series modules and 7 parallel modules. Each module contains 108 series cells and 4 parallel cells.



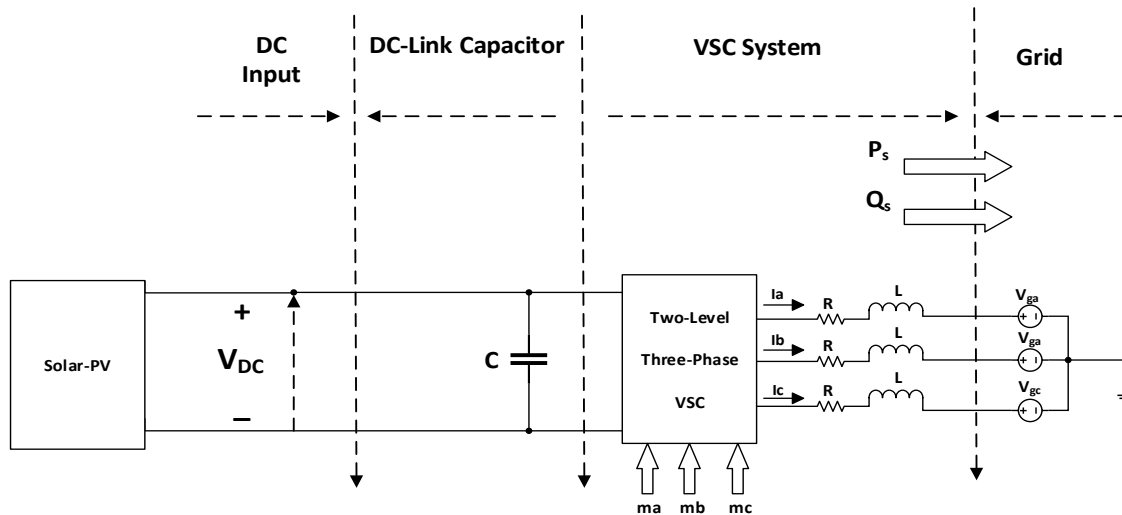


Figure 1. Schematic diagram of grid-following VSC model

2.2. DC capacitor-link

The DC capacitor-link is a large size capacitor which is parallel-connected with the VSC in the solar-PV source side. The main objective of this connection is to minimize the ripples of the solar-PV arrays' output current and enhance the power quality [7]. The capacitance of this capacitor can be determined using equation (1) [8]:

$$C_{dc} = \frac{2P_{max}}{f(V_{DC})^2(1-k^2)}, \quad (1)$$

$$k = \frac{V_{DC.min}}{V_{DC}} \quad (2)$$

where P_{max} represents the solar-PV arrays' maximum output power, V_{DC} is the voltage across the DC capacitor-link, and f represents the system frequency.

According to equations (1) and (2), the value of the capacitor is determined by (1700 μ F) depending on the following values: ($P_{max} = 50$ kW, $f = 50$ Hz, $V_{dc} = 1340$ V and $V_{dc.min} = 800$ V).

2.3. Two-Level Three-Phase VSC

The two-level three-phase VSC consists of three similar half-bridge inverters [5]. Its switched model represents the realistic case of the VSC as it deals with its dynamics and steady-state behaviour. This model relies on the switching functions of the transistors, so the instantaneous values of the output variables can be calculated containing its harmonic components. The switched model of a two-level three-phase VSC consisting of 6 IGBTs combined with snubber circuits. Each leg of the VSC has two switches. The transistors' gating signals are produced using sinusoidal pulse width modulation (SPWM) method as shown in figure 2. This technique depends on comparing the modulating signal (m_a , m_b and m_c) that are produced from the controller with high frequency carrier signals to produce the switching pulses. When the modulating signal is higher than the carrier signal, the comparator generates (1), otherwise it generates (0). The output values from the comparator are the switching signals g_1 , g_3 and g_5 and their complementary represent the switching signals g_4 , g_6 and g_2 , respectively [9].

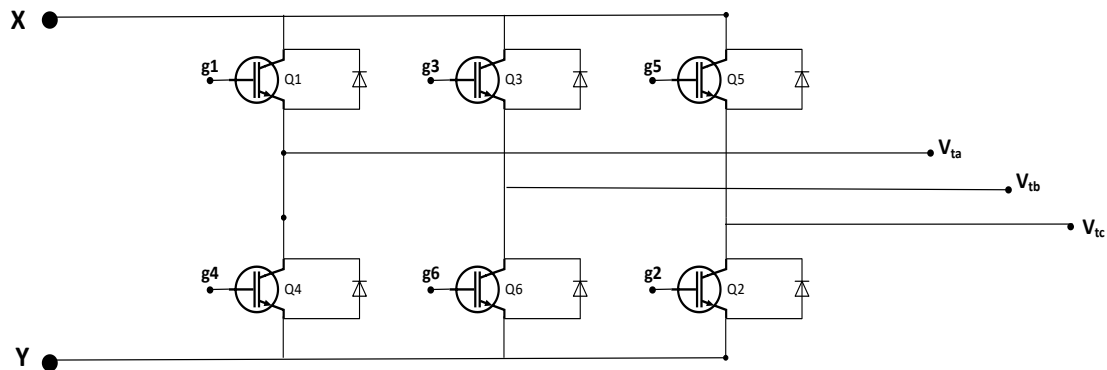


Figure 2. Model of two-level three-phase VSC

2.4. Utility grid

In this system, the utility grid or the AC system is presented by a balanced three-phase sinusoidal voltage source with phase voltage equals 220V and frequency equals 50Hz. Figure 3 clarifies the grid output voltage.

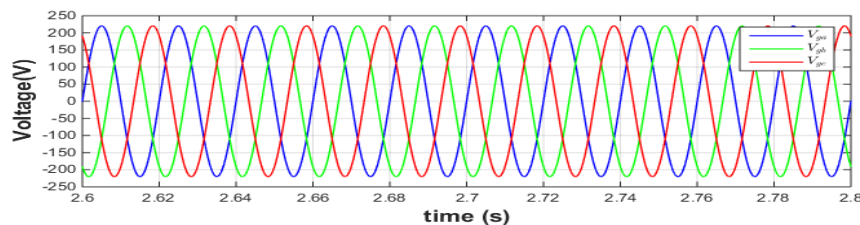


Figure 3. Grid voltage representation

3. Current-control mode (CCM)

The control process of the grid-following VSC is performed using an active/reactive-power-controller. The objective of this controller is to adapt the instantaneous powers that transfer between the VSC and the grid. To facilitate the controller design and simulation, the quantities in abc-frame are transferred into dq0-frame. The main function of this transformation is to decrease the number of control loops from three to two.

In the CCM, the control of the instantaneous active and reactive-power is proceeded using the VSC line current's phase shift and amplitude, simultaneously. Due to the dependence on the VSC line currents in control and regulation scheme, the system is protected from the over-current and faults problems. This control approach is characterized by its high accuracy in controlling the current and its high performance in dealing with harmonics [6]. For these reasons, it's preferred to be chosen and implemented in the presented system model. Figure 4 shows a schematic diagram of a current-controlled grid-following VSC system. In this model, to regulate the active and reactive power, the three-phase VSC output currents and grid voltages are transferred from abc-to-dq0 frame to produce the control signals, i.e. i_d , i_q , V_d , V_q , respectively. These signals are processed using a compensator to generate the control signals of the VSC, i.e. the modulation signals.

3.1. Phase-Locked loop (PLL)

The synchronization between the VSC currents and grid voltage is performed depending on the determination of the grid voltage's phase angle [10], [11]. The value of this phase angle is important in transforming the VSC output current from abc-to-dq0 frame to facilitate the system's control, simplify the compensator design, and decrease the steady-state errors. In this model the synchronization is performed using the phase-locked loop (PLL) method which follow quickly the variations in the grid phasing. The PLL component generates the synchronization angle (ρ) that is used in the transformation

of the system parameters from abc-frame to dq0-frame. The operating concept of the PLL is clarified as follows: when $\rho(t) = \omega_o(t) + \theta_o$, the values of $V_{gd} = \hat{V}_g \cos(\omega_o t + \theta_o - \rho) = \hat{V}_g$ and $V_{gq} = \hat{V}_g \sin(\omega_o t + \theta_o - \rho) = 0$ are DC values which means that the synchronization is performed. Thus, the benefit of connecting a PLL mechanism is achieved, such that it regulates V_{gq} at zero.

The value of the angle (ρ) is reset back to zero once its value reaches (2π) . To ensure that the PLL system is working correctly, the outputs of the abc-to-dq0 frame transformation block are two values such that the value of the d-component equals the peak value of input signal and the value of the q-component equals zero; this is illustrated in the PLL schematic diagram that is presented in figure 5.

3.2. Reference Signal Generator

The function of the reference signal generator block is that it produces the reference control signals, such that, $i_{d_ref}(t)$ and $i_{q_ref}(t)$ depending on the required reference active and-reactive power $P_{s_ref}(t)$ and $Q_{s_ref}(t)$, respectively. These powers are exchanged between the VSC and the grid at common-coupling point (CCP). Thus $P_s(t)$ and $Q_s(t)$ are controlled by the value of i_d and i_q , as follows:

$$i_{d_ref}(t) = \frac{2}{3V_{gd}} P_{s_ref}(t), \tag{3}$$

$$i_{q_ref}(t) = -\frac{2}{3V_{gd}} Q_{s_ref}(t). \tag{4}$$

The control system must track these reference signals, such that, $i_d \approx i_{d_ref}$ and $i_q \approx i_{q_ref}$, so the generated real and reactive power follow their reference values, that is, $P_s \approx P_{s_ref}$ and $Q_s \approx Q_{s_ref}$.

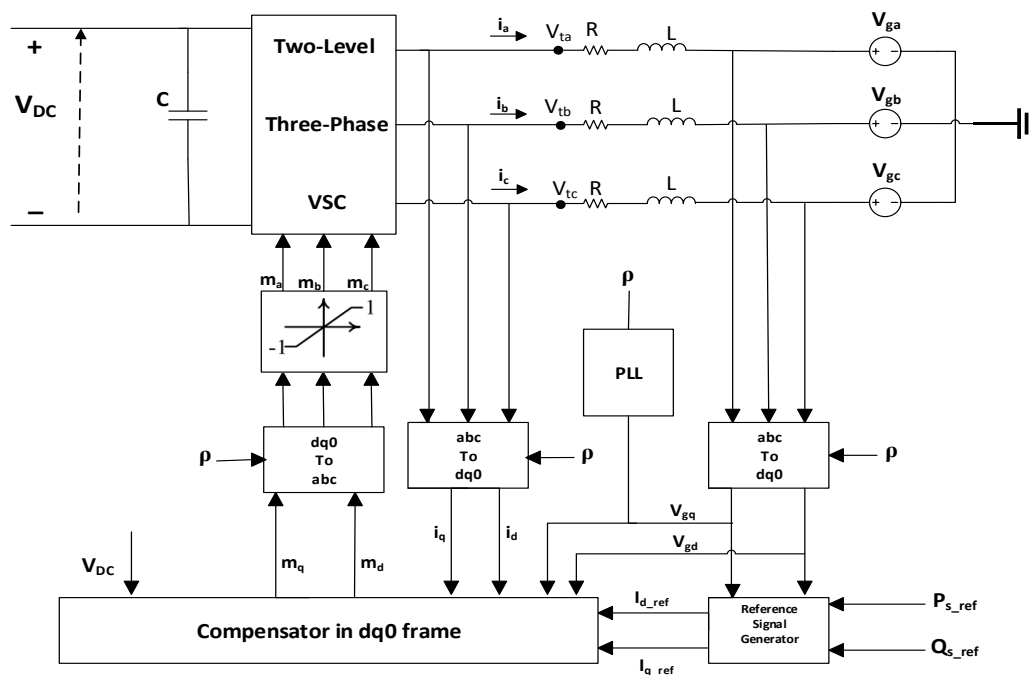


Figure 4. Schematic diagram of current-controlled grid-connected VSC system

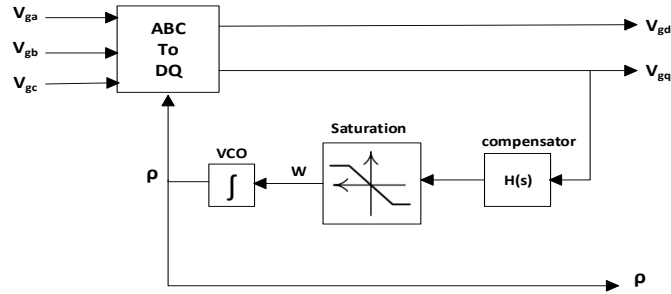


Figure 5. PLL schematic diagram

3.3. Compensator

The compensator block shown in figure 5 is used to generate the modulating signals of the VSC. In the proposed controller, the VSC output current signals (i_a , i_b and i_c) are used as input signals to the compensator after transforming them from abc-to-dq0 frame. Then the current signals i_d and i_q are compared with the reference control signals, such that, i_{d_ref} and i_{q_ref} which generated from the reference signal generator as mentioned before. Also, the utility grid voltages are transformed from abc-to-dq0 frame to produce V_{gd} and V_{gq} that are fed to the compensator as input signals. These compensator's input signals are used in the control system to generate the modulating signals of the VSC in dq0-frame and then they are transformed again into abc-frame and injected into the VSC to produces the IGBTs' switching pulses. The equations that explain the compensator design and its control loops are presented in the following. The dynamics of the grid-connected VSC can be described as:

$$\vec{V}_t = L \frac{d\vec{i}}{dt} + \vec{i}R + \vec{V}_g(t), \quad (5)$$

then substituting for $\vec{V}_t = V_{tdq} e^{j\rho}$, $\vec{i} = i_{dq} e^{j\rho}$ and the space phasor form of the grid voltage is $\vec{V}_g(t) = \hat{V}_g e^{j(\omega_o t + \theta_o)}$. Equation (5) can be written:

$$V_{tdq} e^{j\rho} = L \frac{d}{dt} (i_{dq} e^{j\rho}) + (i_{dq} e^{j\rho})R + \hat{V}_g e^{j(\omega_o t + \theta_o)}, \quad (6)$$

by differentiation, then $L \frac{d}{dt} (i_{dq} e^{j\rho}) = L e^{j\rho} \frac{di_{dq}}{dt} + jL i_{dq} e^{j\rho} \frac{d\rho}{dt}$, substitution and multiplication all terms in equation (6) by $(e^{-j\rho})$,

$$V_{tdq} = L \frac{d(i_{dq})}{dt} + jL i_{dq} \frac{d(\rho)}{dt} + (i_{dq})R + \hat{V}_g e^{j(\omega_o t + \theta_o - \rho)}, \quad (7)$$

Equation (7) can be decoupled into two equations (real and imaginary), such as $f_{dq} = f_d + jf_q$.

Considering steady-state conditions in the proposed control system, then after substituting for $V_{gd} = \hat{V}_g \cos(\omega_o t + \theta_o - \rho)$, $V_{gq} = \hat{V}_g \sin(\omega_o t + \theta_o - \rho)$ and $\omega(t) = \omega_o$ in equation (7), then:

$$L \frac{d(i_d)}{dt} = L \omega_o i_q - (R)i_d + V_{td} - V_{gd}, \quad (8)$$

$$L \frac{d(i_q)}{dt} = -L \omega_o i_d - (R)i_q + V_{tq} - V_{gq}, \quad (9)$$

from the VSC averaged model presented in [5], [12], the relation between the two-level VSC's AC-side voltage and the modulating signal can be expressed as follows:

$$\vec{V}_t(t) = \frac{V_{DC}}{2} \vec{m}(t), \quad (10)$$

then equation (10) can be transformed in its dq0-frame components and presented, such that:

$$V_{td}(t) = \frac{V_{DC}}{2} m_d(t), \quad (11)$$

$$V_{tq}(t) = \frac{V_{DC}}{2} m_q(t), \tag{12}$$

by substituting for equations (11) and (12) into equations (8) and (9) respectively, the expression of the modulating signals into dq0-frame will be generated as follows:

$$m_d = \frac{2}{V_{DC}} (u_d - L \omega_o i_q + V_{gd}), \tag{13}$$

$$m_q = \frac{2}{V_{DC}} (u_q + L \omega_o i_d + V_{gq}), \tag{14}$$

where, u_d and u_q are new control signals, and their values can be deduced as:

$$u_d = L \frac{d(i_d)}{dt} + (R) i_d, \tag{15}$$

$$u_q = L \frac{d(i_q)}{dt} + (R) i_q. \tag{16}$$

Based on the previous equations, the VSC current controller presented in dq0-frame is shown in figure 6, in which there are two compensators. The first one is the d-component compensator that processes $e_d = i_{d-ref} - i_d$ and produces u_d that participate in generating m_d . Similarly, the second is the q-component compensator that processes $e_q = i_{q-ref} - i_q$ and produces u_q that participates in generating m_q . Then m_d and m_q are multiplied by $(V_{DC}/2)$ to generate V_{td} and V_{tq} that control i_d and i_q , respectively. The values of k_d and k_q are identical and can be simply presented by a proportional-integral (PI) controller. The values of these compensators can be determined depending on the following equations [12]:

$$k_d(s) = k_q(s) = \frac{k_p(s) + k_i}{s}, \tag{17}$$

Where: $k_p = \frac{L}{\tau_i}$, $k_i = \frac{R}{\tau_i}$, and τ_i is the closed-loop system's requested time constant and its value ranges between 0.5-5 m sec.

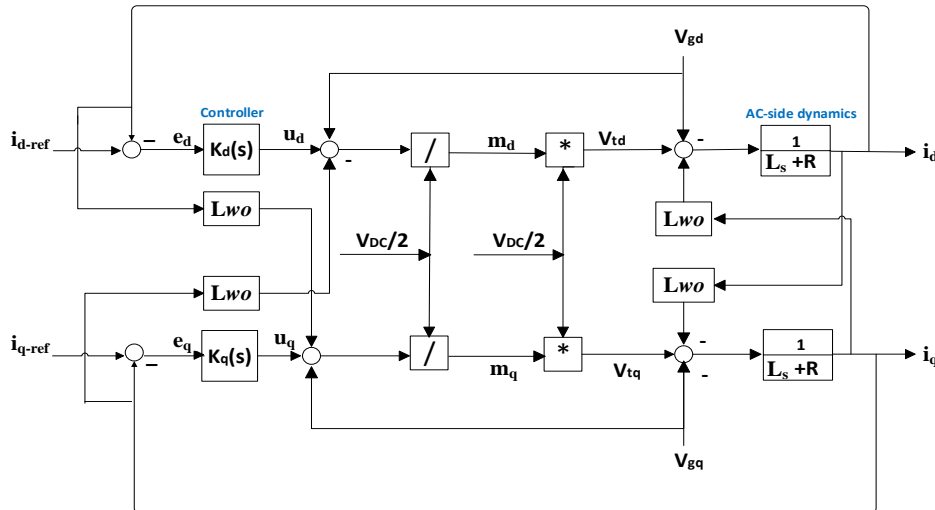


Figure 6. Current-control mode of VSC system in dq0-representation

4. Case study results

The system under study is completely modelled and simulated using PSCAD/EMTDC software. The instantaneous reactive and active powers transferred from the VSC to the utility grid are controlled using the CCM method. The control system is composed of many components and blocks as mentioned before. The performance of these blocks is presented as follows.

4.1. PLL model

The frequency range of the PLL should be selected within a cramped domain of variations and also, it should be sufficiently wide to allow deviations of $\omega(t)$ through transients and quickly respond to disturbances. Its range is chosen between 35 Hz and 65 Hz. PLL's start-up transients are shown in figure 7. It is obvious that, before $t = 0.06 \text{ sec}$, the voltage V_{gd} and V_{gq} are time-variant values, as the output frequency from the PLL's compensator is saturated at $f_{min} = 35 \text{ Hz}$. At $t = 0.06 \text{ sec}$, the voltage V_{gd} is decreased and directed toward zero, so the compensator increases the frequency value. At $t = 0.12 \text{ sec}$, the PLL works perfectly and generates DC quantities such that $V_{gd} = \hat{V}_g$, V_{gq} is regulated at zero. Also, the same figure shows that the synchronization is performed such that the value of angle (ρ) is reset back to zero once its value reaches (2π) .

The transformation from abc-to-dq0 is executed using the Park transformation matrix [13]. The grid voltage and the VSC output current signals are transformed from abc-to-dq0 frame, and then they are injected into the compensator to be processed. Figure 8 shows the transformation of the grid voltage to dq0-frame where $V_{gd} = \hat{V}_g = 220 \text{ V}$ and $V_{gq} = \text{Zero}$. Also, the VSC's output currents represented in dq0-frame are shown in figure 9, where $i_d = \hat{i}_a \cong 152.5 \text{ A}$ and $i_q \cong \text{Zero}$. As the active and reactive powers' initial condition equal zero, the value of $i_d = \text{zero}$, for $t \leq 0.2 \text{ sec}$.

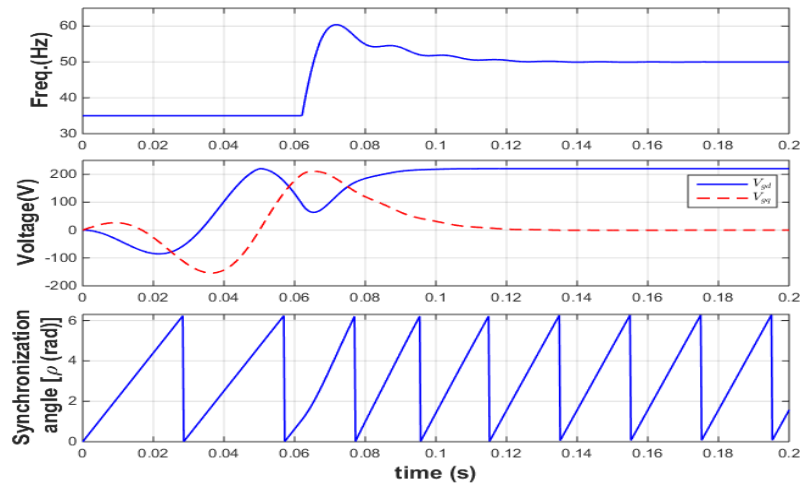


Figure 7. PLL's start-up response

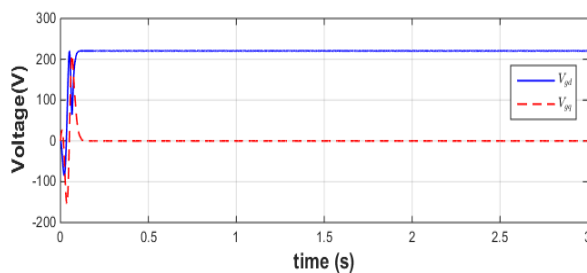


Figure 8. Grid voltage in dq0-frame

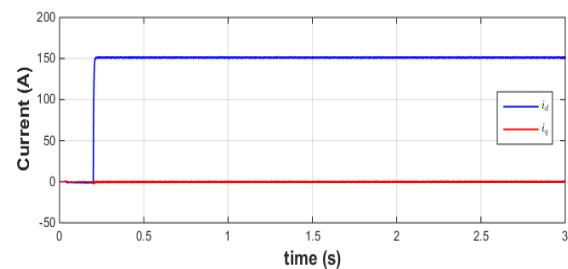


Figure 9. VSC's output current in dq0-frame

4.2. Reference signal generator model

The inputs to this block are the reference values for the required active and reactive powers (P_{s-ref} and Q_{s-ref}), where the outputs are the reference dq-components of the VSC's output currents such that i_{d-ref} and i_{q-ref} according to equations (3) and (4). Then these values are injected to the compensator and compared with the dq-components of the VSC's output currents such that i_d and i_q where the control system must track these reference signals as illustrated in figure 10. The value of current i_q ranges between (1.5 A, -1.5 A), which is due to the residual harmonics after insertion of an LCL filter. Also, its

value increased to 3A at $t = 0.2 \text{ sec}$, due to the changing of the system's conditions from its initial values ($P_{s\text{-ref}} = \text{zero}$ and $Q_{s\text{-ref}} = \text{zero}$) to its designed values ($P_{s\text{-ref}} = 50 \text{ kW}$ and $Q_{s\text{-ref}} = \text{zero}$).

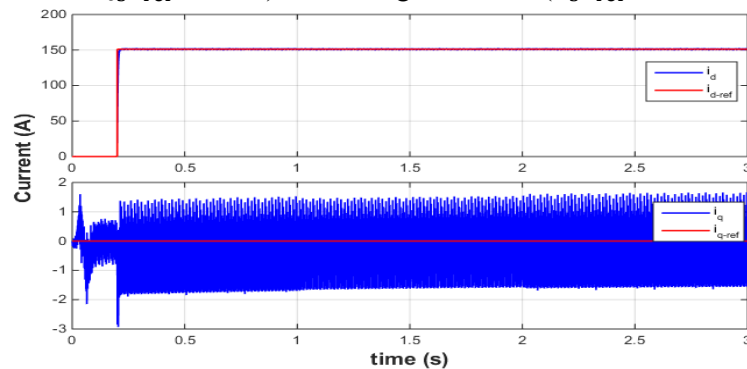


Figure 10. Tracking of the dq0-components of the VSC's output current with their reference values

4.3. The compensator model

The compensator's input signals are the VSC output current signals in dq0-frame (i_d and i_q), the grid voltage signals in dq0-frame (V_{gd} and V_{gq}), the output signals from the reference signal generator block ($i_{d\text{-ref}}$ and $i_{q\text{-ref}}$) and the solar-PV output DC voltage. The compensator output signals are the modulating signals of the VSC in dq0-frame (m_d and m_q), then they are fed to a limiter so their values are limited between (1,-1), after that they are transformed again into abc-frame (m_a , m_b and m_c) and injected to the VSC to produce the IGBTs' gating signals. Depending on equation (17) with the time constant value $\tau_i = 2.5 \text{ m sec}$, the design values of the used PI controller's parameters are $k_p = 4.02 \Omega$ and $k_i = 2.352 \Omega/\text{sec}$ (by taking into account the values of LCL-filter's parameters). The generated modulating signals in abc-frame are shown in figure 11, where they are sinusoidal signals with amplitude ranges between (-1,1).

Finally, the proposed VSC controller regulates the active and reactive powers ($P_s(t)$ & $Q_s(t)$) which transferred from the solar-PV arrays to the utility grid through the VSC, as illustrated in figure 12. It is clear that the produced active and reactive powers track their reference values that are adjusted to be $P_{s\text{-ref}} = 50 \text{ kW}$ and $Q_{s\text{-ref}} = \text{zero}$, respectively. It is clear that the value of output reactive power doesn't equal zero and ranges between about (-500 VAR, 500 VAR), this is due to the residual harmonics after implementation of an LCL filter. According to "The Egyptian Solar Energy Plants Grid Connection Code" [14], the power factor value of the transferred power from the VSC to the grid should be within the limit (0.95 lagging, 0.95 leading). The power factor of the system is about 0.999 lag, therefore the value of the generated reactive power is acceptable.

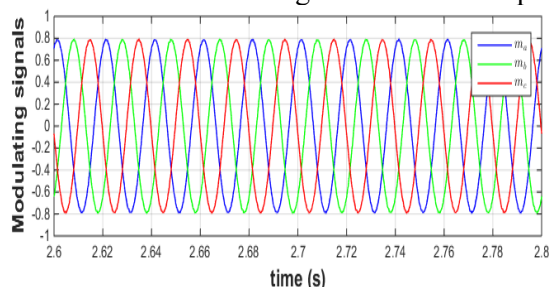


Figure 11. VSC's modulating signals in abc-frame

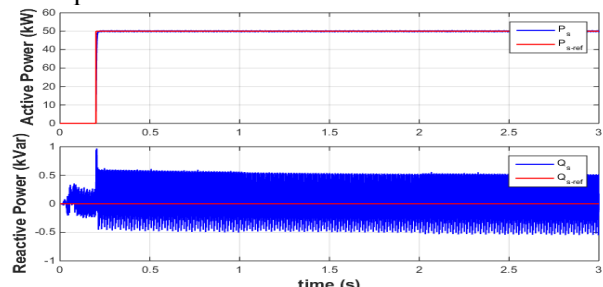


Figure 12. Tracking of the generated active and reactive powers with their reference values

5. Conclusion

This paper proposed a step by step designing and control of a grid connected, three phase, two level VSC has been presented using PSCAD /EMTDC software. The control of the VSC is performed based on the grid following VSC methodology. In order to control the instantaneous transferred active and reactive power between the VSC and the grid, CCM (dq0) frame is used. Based on the implemented model the power that transferred from the VSC to the grid track the initial conditions of the required power, so the control technique achieves the required task.

References

- [1] Sayigh A 2012 *Solar energy engineering*: Elsevier
- [2] Kumar N M, Subathra M P and Moses J E 2018 On-grid solar photovoltaic system: Components, design considerations, and case study. In: *2018 4th International Conference on Electrical Energy Systems (ICEES)*: IEEE pp **616-9**
- [3] Kalbat A 2013 PSCAD simulation of grid-tied photovoltaic systems and Total Harmonic Distortion analysis. In: *2013 3rd International Conference on Electric Power and Energy Conversion Systems*: IEEE pp **1-6**
- [4] Saad E, Elkoteshy Y and AbouZayed U 2020 Modelling and analysis of grid-connected solar-PV system through current-mode controlled VSC. In: *E3S Web of Conferences*: EDP Sciences p 05005
- [5] Rashid M H 2017 *Power electronics handbook*: Butterworth-Heinemann)
- [6] Kazmierkowski M P and Malesani L 1998 Current control techniques for three-phase voltage-source PWM converters: A survey *IEEE Transactions on industrial electronics* **45** 691-703
- [7] Rahman S A and Varma R K 2011 PSCAD/EMTDC model of a 3-phase grid connected photovoltaic solar system. In: *2011 North American Power Symposium*: IEEE pp **1-7**
- [8] Chatterjee K, Fernandes B and Dubey G K 1999 An instantaneous reactive volt-ampere compensator and harmonic suppressor system *IEEE transactions on power electronics* **14** 381-92
- [9] Wu B and Narimani M 2017 *High-power converters and AC drives*: John Wiley & Sons)
- [10] Blaabjerg F, Teodorescu R, Liserre M and Timbus A V 2006 Overview of control and grid synchronization for distributed power generation systems *IEEE Transactions on industrial electronics* **53** 1398-409
- [11] Sozer Y and Torrey D A 2009 Modeling and control of utility interactive inverters *IEEE Transactions on Power Electronics* **24** 2475-83
- [12] Yazdani A and Iravani R 2010 *Voltage-sourced converters in power systems* vol **39**: Wiley Online Library
- [13] Krause P C, Wasynczuk O, Sudhoff S D and Pekarek S 2002 *Analysis of electric machinery and drive systems* vol **2**: Wiley Online Library
- [14] <http://egyptera.org/ar/Code.aspx>